sustainability

MDPI

Article

Buriti Fabric Reinforced Epoxy Composites as a Novel Ballistic Component of a Multilayered Armor System

Luana Cristyne da Cruz Demosthenes, Fernanda Santos da Luz *, Lucio Fabio Cassiano Nascimento and Sergio Neves Monteiro

Department of Materials Science, Military Institute of Engineering—IME, Praça General Tibúrcio 80, Urca, Rio de Janeiro 22290-270, Brazil

* Correspondence: fsl.santos@gmail.com

Abstract: Buriti Fibers extracted from the leafstalk of palm tree, *Mauritia flexuosa*, native to the Amazon region, have been investigated as a reinforcement of polymer matrix composites. Recently, the fabric made from buriti fibers was also studied as a possible reinforcement of epoxy composites. In particular, the preliminary results of a 10 vol% buriti fabric epoxy composite in a multilayered armor system (MAS) displayed a satisfactory backface signature (BFS) but the composite target was not able to preserve its integrity after the ballistic impact. This motivated the present work, in which we carry out a complete statistical investigation of the ballistic performance of 10, 20, and 30 vol% buriti fabric epoxy composites as a MAS second layer against 7.62 mm rifle ammunition. BFS, associated with the depth of penetration in a clay witness simulating a human body, disclosed values of 18.9 to 25 mm, statistically similar and well below the lethal value of 44 mm specified by the international standard. Absorbed energy in stand-alone ballistic tests of 163–190 J for armor perforation were also found to be statistically higher than 58 ± 29 J obtained for the conventionally applied synthetic aramid fabric. The 30 vol% buriti fabric composites maintained the integrity of the MAS second layer, as required for use in body armor. Failure mechanisms found for the 10 vol% and 20 vol% buriti fabric composites by macro analysis and scanning electron microscopy confirmed the importance of a higher amount such as 30 vol% in order to achieve effective ballistic protection.

Keywords: buriti fabric; epoxy composite; multilayered armor; ballistic test

check for updates

Citation: Demosthenes, L.C.d.C.; Luz, F.S.d.; Nascimento, L.F.C.; Monteiro, S.N. Buriti Fabric Reinforced Epoxy Composites as a Novel Ballistic Component of a Multilayered Armor System. *Sustainability* **2022**, *14*, 10591. https://doi.org/10.3390/su141710591

Academic Editor: Anastasia V. Penkova

Received: 22 July 2022
Accepted: 19 August 2022
Published: 25 August 2022

Publisher's Note: MDPI stays neutral with regard to jurisdictional claims in published maps and institutional affiliations.

Copyright: © 2022 by the authors. Licensee MDPI, Basel, Switzerland. This article is an open access article distributed under the terms and conditions of the Creative Commons Attribution (CC BY) license (https://creativecommons.org/licenses/by/4.0/).

1. Introduction

The sustainable destination of hazardous wastes [1,2], as well as protection against electromagnetic waves [3–7] and firearm thread [8–10], are among the increasing human challenges faced by our society and have most recently been tackled in particular during armed conflicts.

Armed conflicts have raised considerable attention due to the escalating level of firearm threat against both policemen and military personnel. Adequate protection is necessary to prevent trauma from increasingly heavy caliber ammunitions. This has motivated researchers to develop more efficient personal protection such as the multilayered armor system (MAS), which is composed of distinct layers of materials to resist the impact of high supersonic velocity (>800 m/s) projectiles [11,12]. The first layer is a hard and brittle ceramic, which not only fragments but also erodes the projectile, dissipating most of the ballistic impact energy [13]. The second layer is a material with a lower density than the ceramic to reflect the impact compressive wave as a tensile wave and cause front ceramic fragmentation. This MAS second layer also absorbs a significant amount of remaining energy associated with the cloud of ceramic and projectile fragments [14]. In addition to conventional synthetic materials such as aramid fabric (Kevlar or Twaron), which for long time have been applied as a MAS second layer [15], natural lignocellulosic fiber (NLF) composites have recently been considered as promising alternatives [16–19].

Polymer composites reinforced with NLFs have become, since the beginning of this century, an important alternative to replace synthetic fiber composites such as fiberglass [20,21]. Indeed, NLF composites present favorable advantages such as lower density, cost effectiveness and less abrasion to process equipment, as well as a diversified kind of natural fiber and fabrics [22–25]. These composites have motivated numerous applications related to automobile parts [26], panels for building construction [27] and ballistic hard armor [28].

Several NLFs endemic in the Amazon region of South America such as curaua, carnauba, guaruman, tucum, caranan and buriti have been considered as reinforcements for polymer composites. Among these NLFs, the fiber extracted from the leafstalk of the *Mauritia flexuosa* palm tree, known as buriti and illustrated in Figure 1, has been investigated in composites [29–44] for more than a decade. This Amazon palm tree can reach about 30 m in height with a 50 cm thick stem (Figure 1a). Its leaves are used as coverings for houses or art crafts, such as hammocks, ropes, and hats. The leafstalk (petiole) can reach 3 m in length, Figure 1b, and its fibers are high in cellulose (77.8%) and low in lignin 24.0% contents [45]. These fibers are extracted from the petiole's epidermis and can be used to produce mats and curtains. In addition, the inner and spongy part of the petiole is used in handicrafts, such as decorative pieces, as well as toys and bottle stoppers [46].

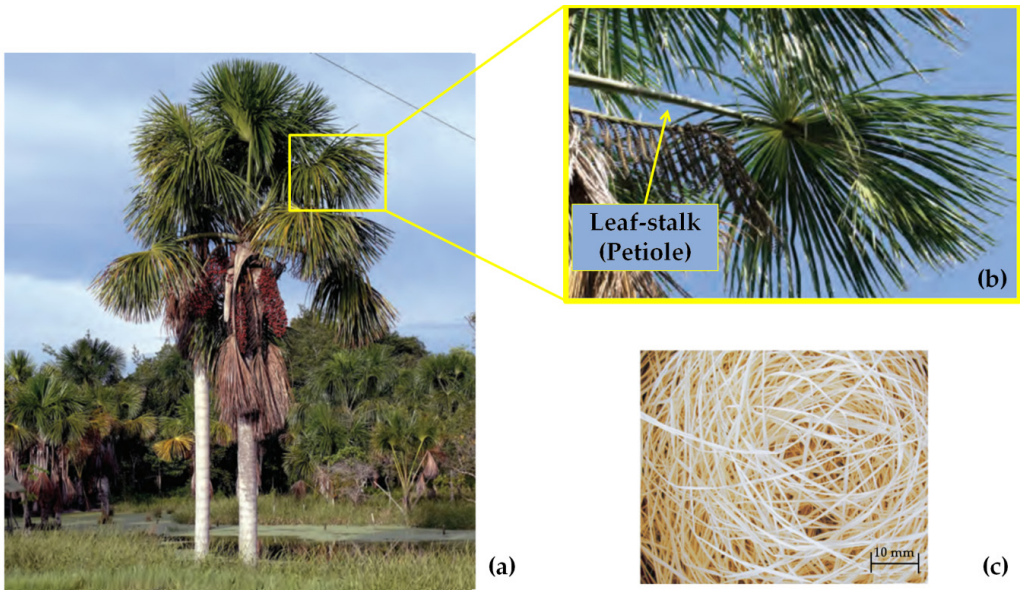

Figure 1. Buriti *Mauritia flexuosa*: (**a**) palm tree; (**b**) leaf-stalk (petiole); and (**c**) bundle of extracted fibers (adapted from Demosthenes et al. [32]).

The relatively low density, 0.63–1.12 g/cm^3, and moderate tensile strength, 129 to 254 MPa, of buriti fibers make them appropriate reinforcement for less dense but relatively weaker polymer composites [47].

However, only recently superior ballistic performances were disclosed regarding Amazon NLF polymer composites, especially in curaua [48–51] as well as guaruman [52] and tucum [53]. In particular, a preliminary work [54] on 10 vol% buriti fabric reinforced epoxy composites revealed promising results as a MAS second layer against high velocity level III NIJ [55] ammunition. Table 1 compares the ballistic performance of both synthetic fabrics and natural fabrics reinforced polymer composites as a MAS second layer with the same thickness (~10 mm). A comparison is made in terms of indentation depth caused by a 7.62 mm projectile impact against a clay witness simulating a human body. However, this buriti fabric composite was not able to keep its integrity after the 7.62 mm projectile impact. In practice this constitutes a ballistic failure in a multi-hit test, which requires the MAS second layer to be an integer after six shootings, as per NIJ standard [55].

Table 1. Comparison between the ballistic the ballistic performance of both synthetic fabrics and natural fabrics reinforced polymer composites as the MAS second layer with the same thickness.

MAS Second Layer	Depth of Indentation (mm)	Reference
Aramid fabric/Kevlar™	21 ± 3	[56]
Ultra-high molecular weight polyethylene non-woven fabric/Dyneema™	41 ± 2	[57]
10 vol% buriti fabric/epoxy	22 ± 4	[54]
30 vol% curaua non-woven fabric/epoxy	28 ± 3	[58]
30 vol% jute fabric/epoxy	21 ± 3	[59]

As a MAS second layer, the lower the indentation depth, the better the ballistic performance. A depth higher than 44 mm is considered a lethal trauma [55].

Although many NFLs have been investigated as a reinforcement of polymer composites for the MAS second layer [16–18,28,48–53], new relevant results on buriti fabric will be disclosed in the present work. Indeed, uniquely obtained from a native Brazilian Amazon palm tree, buriti fabric is, for the first time, successfully investigated in composites with a relatively larger amount of 30 vol%, which might be considered an innovation for effective use by the national armed forces. Moreover, particularly improved results are revealed in comparison with the ballistic performance of polymer composites reinforced not only with other NLFs but also synthetic fabrics.

Based on the possible ballistic failure reported on the preliminary investigated composite [54] to be a consequence of the relatively small amount of buriti fabric, the present work evaluates the performance of epoxy composites with up to 30 vol% of buriti fabric. Ballistic tests with these novel composites with a higher volume fraction of buriti fabric, also as the MAS second layer, were carried out under similar threat of 7.62 ammunition. A thorough ANOVA statistical evaluation of the depth of penetration in a clay witness simulating a human body, as well as a macro analysis and scanning electron microscopy observations, were performed to verify the composites' integrity.

2. Materials and Methods

2.1. Composite Manufacturing

Buriti fabric was purchased at the Adolpho Lisboa municipal market in the city of Manaus, State of Amazonas, north of Brazil. Figure 2a illustrates the actual buriti fabric manually made with plain weave by the indigenous community in the interior of Amazonas. The microscopic aspect of this weave, by scanning electron microscopy (SEM), can be observed in Figure 2b. The as-received fabric was cut in rectangular pieces of 120 × 150 mm and dried in a stove at 60 °C for 24 h to release surface moisture. The complete thermal and structural characterizations of the buriti fabric composites can be found elsewhere [32]. For composite manufacturing, the average density of the buriti fabric was considered as 0.911 g/cm^3 [40] and for DGEBA/TETA epoxy was 1.11 g/cm^3 [60].

Composite epoxy plates with 10, 20, and 30 vol% of buriti fabric were produced using commercial diglycidyl ether of the bisphenol-A (DGEBA) epoxy resin mixed with hardener triethylenetetramine (TETA) in a stoichiometric ratio of 13 parts per 100 of resin, both supplied by Epoxyfiber, Rio de Janeiro, Brazil. Figure 2c shows a scheme of the composite manufacturing process. This process involves pouring a still fluid epoxy into a metallic mold intercalated with the buriti fabric pieces in amounts corresponding to the desired volume fractions and calculated by the fabric and resin densities. Then, the mold is closed, and the composite is cured at room temperature under a pressure of 3 MPa for 24 h.

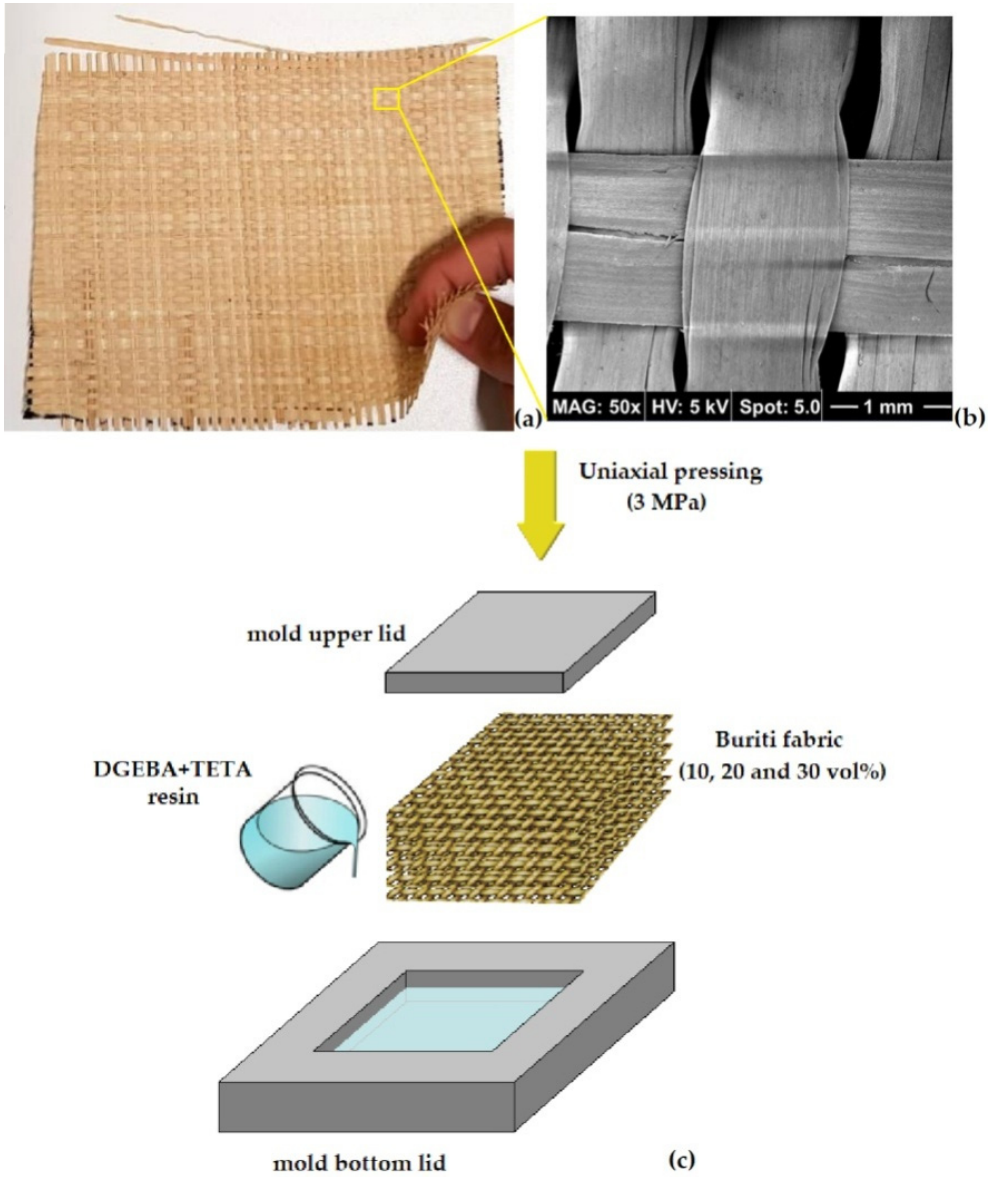

Figure 2. (**a**) Manually made plain weave buriti fabric and (**b**) SEM detail of the plain weave (adapted from Demosthenes et al. [32]); (**c**) scheme of composite manufacturing process.

2.2. Ballistic Tests

To evaluate the ballistic performance, two distinct ballistic tests were carried out at the Army Assessment Center (CAEx), Rio de Janeiro, Brazil, using level III 7.62 × 51 mm caliber projectile with 9.7 g of mass shot from a gun barrel with velocity of 838 ± 15 m/s. The first type of ballistic test used a MAS target, shown in Figure 3, backed by a block of clay witness simulating a human body. The clay, supplied by Corfix, Porto Alegre, Brazil, was compressed to avoid air bubbles and kept at 29 °C for at least 3 h to acquire the plasticity and density required by the standard [55]. After the ballistic test, a laser sensor measured the indentation depth in the clay witness, known as backface signature (BFS), which simulates the trauma caused to the MAS wearer by the projectile impact. A BFS equal or superior to 44 mm is considered as a lethal trauma and, consequently, the failure of the MAS protection [55].

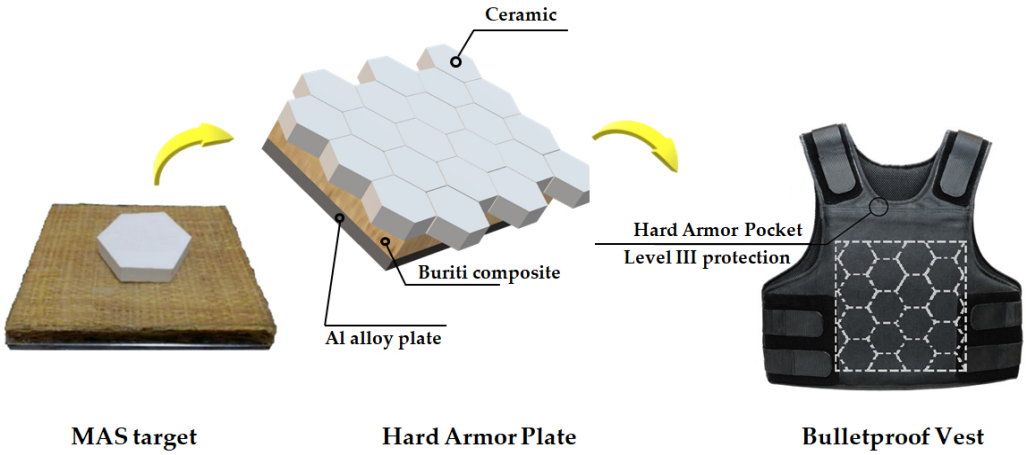

Figure 3. Multilayered armor system (MAS) used as sample in ballistic tests and the hard armor plate proposed to be inserted in a bulletproof vest.

The MAS applied as the ballistic target in this study was assembled with the conventional thickness of 25 mm (∼one inch) in a hard armor plate to be inserted in a bulletproof vest for protection against level III ammunition [55]. An actual MAS target sample and the scheme of the hard armor plate is shown in Figure 3.

In this figure, the front layer, the first hit by the projectile, is a 10 mm thick hexagonal alumina (Al_2O_3) ceramic tile doped with 4 wt% of niobia (Nb_2O_5), processed by sintering at 1400 °C, as reported elsewhere [61]. The MAS second layer in Figure 3 is the 10 mm thick buriti fabric composite plate. The final back layer in Figure 3 is a 5 mm thick sheet of 5052-H34 aluminum alloy with same lateral dimensions of 150 × 120 mm as the composite plate. Figure 4 shows a scheme of the CAEx standard ballistic shooting line set up with inserted pictures of: (a) gun barrel; (b) MAS target and clay witness; and (c) BFS measurement with a model Q4X Banner laser sensor.

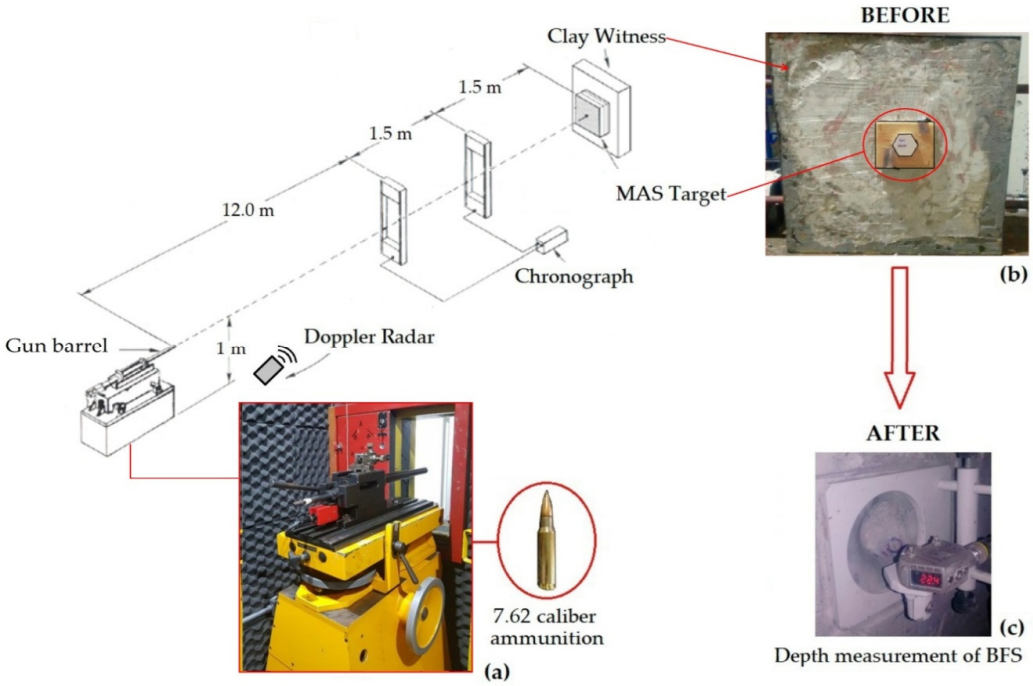

Figure 4. Scheme of the CAEx standard ballistic shooting line: (**a**) gun barrel; (**b**) MAS target and clay witness; and (**c**) BFS measurement with a model Q4X Banner laser sensor.

The second type of ballistic test is known as "stand-alone", in which the target is solely the composite plate. In the stand-alone test, a single composite plate, without the ceramic front layer, is perforated by the high impact energy of the level III 7.62 mm ammunition. In this case, both impact velocity (v_i) and the residual (v_r) of the projectile leaving the plate after perforation are measured by the Doppler radar and optical barrier shown in Figure 4. Then, the absorbed ballistic impact energy (E_{abs}) of the composite plate is estimated by:

$$E_{abs} = \frac{m_p \cdot (v_i^2 - v_r^2)}{2}, \quad (1)$$

where m_p is the mass of the projectile (9.7 g) and v_i and v_r are the impact and residual velocities, respectively.

In addition, through the stand-alone test, another important parameter, limit velocity (V_L), which corresponds to the highest projectile velocity without target perforation, can be obtained. According to Morye et al. [62], V_L is a reference for the maximum level of ammunition that can be withstood by the polymer composite target as an effective armor and is given by:

$$V_L = \sqrt{\frac{2 \cdot E_{abs}}{m_p}} \quad (2)$$

2.3. Statistical Analysis

To statistically compare values of averages and corresponding standard deviations, analysis of variance (ANOVA) was applied to the results obtained in both types of ballistic tests in order to assess whether there was a significant difference between the data. The ANOVA 95% confidence level was adopted, where the alternative hypothesis is assumed by comparing the calculated F_{calc} with the critical F_{crit}, which is tabulated. If $F_{calc} > F_{crit}$, it is concluded with 95% confidence that there is a difference between the average values: otherwise, if $F_{calc} < F_{crit}$. In case of difference, then the Tukey test, also known as the honest significant difference test (*HSD*), becomes necessary. This test allows a two-by-two comparison of epoxy composites with a different volume fraction of buriti fabric. The hypothesis of equality is determined by the Tukey lower significant difference:

$$HSD = q \cdot \sqrt{\frac{MSR}{r}} \quad (3)$$

where q is a tabulated value that depends on the residual freedom degree and the number of treatments (conditions); *MSR* is the means of square residual; and r is the number of repetitions.

This methodology makes it possible to statistically determine the influence of the volume fraction of buriti fabric in the ballistic results of the epoxy composites.

2.4. Scanning Electron Microscopy (SEM)

The microscopic aspect of the buriti/epoxy composite target after the ballistic impact was analyzed by SEM in a Quanta FEG 250 Fei microscope, operating with secondary electrons between 5 and 15 kV. To avoid electronic charging, before observation, the samples were gold-sputtered in a Leica EM ACE600.

3. Results and Discussion

3.1. Multilayered Armor System (MAS)

Figure 5 illustrates the macro aspect of MAS targets with a ceramic front layer and buriti fabric epoxy composites as the second layer, followed by an Al alloy sheet as the third layer. Figure 5a, similar to Figure 3, shows a complete MAS as the target placed in the shooting line, Figure 4, before the ballistic test. Figure 5b–d show, respectively, the epoxy composites, with 10 vol% (EC10BF), 20 vol% (EC20BF), and 30 vol% (EC30BF) of buriti fabric, corresponding target aspects after the 7.62 mm ballistic impact. In all

tested MAS targets, the front ceramic was totally destroyed as it absorbed most of the impact energy [13] and caused a cloud of fragment to travel through the buriti fabric composite second layer [54]. The behavior of the ceramic layer is explained by the Nb_2O_5 embrittlement, causing an intergranular fragmentation, as reported elsewhere [13,28]. Although the ceramic front layer is responsible for absorbing most of the projectile's impact energy, the second layer in the MAS has another effective mechanism of energy dissipation, which involves capturing ceramic fragments [3], further shown by SEM images.

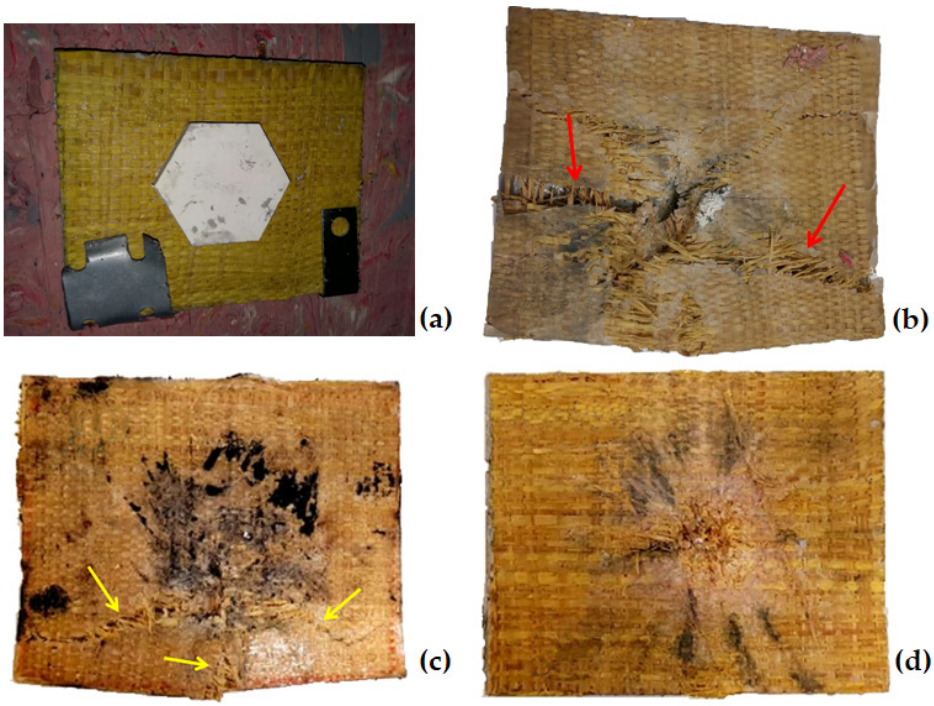

Figure 5. MAS target against level III 7.62 mm ammunition: (**a**) complete with hexagonal front ceramic tile before ballistic test; (**b**) EC10BF after ballistic test; (**c**) EC20BF after ballistic test; and (**d**) EC30BF after ballistic test.

As revealed in Figure 5b, the 10 vol% buriti fabric epoxy composites, as the MAS second layer, were not able to keep their full integrity [54]. Indeed, extensive open rupture regions of failure, indicated by red arrows, discarded the possibility of applying EC10BF as body armor to protect against subsequent shootings as required by the NIJ standard [55].

The 20 vol% buriti fabric epoxy composites after the test, Figure 5c, depict cracks indicated by yellow arrows. Although, apparently not as serious as the rupture of EC10BF in Figure 5b, the EC20BF would not be recommended for the MAS second layer against 7.62 mm ammunition.

Regarding the 30 vol% buriti fabric epoxy composite, Figure 5d, except for localized partial damage caused by the cloud of fragments at the center of the plate, no open failure like in EC10BF, Figure 5b, or piercing cracks like in EC20BF, Figure 5c, are observed. Therefore, a MAS with EC30BF as the second layer could be used as body armor against level III 7.62 mm ammunition.

Table 2 presents the BFS associated with the depth of indentation caused in the clay witness and measured by a laser sensor, Figure 4, for the investigated buriti fabric epoxy composites as the MAS second layer against 7.62 mm ammunition. In this table, all composites display BFS values significantly lower than the lethal trauma of 44 mm specified by the NIJ standard 0101.06 [55]. In spite of the most favorable BFS of 18.9 $\pm$ 1.9 mm, the 10 vol% buriti fabric composites cannot be applied in body armor due to a lack of integrity. Table 2 also reveals a tendency of increasing the value of BFS with the volume fraction of buriti fabric. The validity of this tendency will be further statistically studied by ANOVA.

Table 2. Backface signature (BFS) associated with depth of indentation of epoxy composites reinforced with buriti fabric ballistic tested as MAS second layer against 7.62 mm ammunition.

Composite	BFS (mm)	Reference
EC10BF	18.9 ± 1.9	PW
EC20BF	21.0 ± 1.9	PW
EC30BF	25.0 ± 3.3	PW
Lethal BFS	≥44	[45]

PW: Present work.

In Figure 6, the BFS variation with the volume fraction of buriti fabric in the epoxy composites is presented. The value reported for the plain DGEBA/TETA epoxy plate [59,63] with the same 10 mm thickness as the MAS second layer is also shown in this figure.

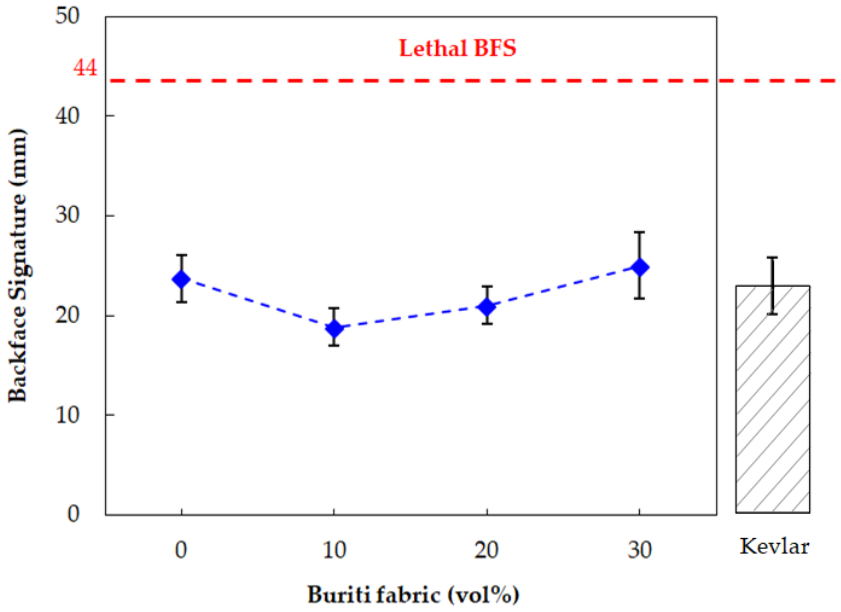

Figure 6. Variation in BFS caused by the impact of a 7.62 mm projectile, with the volume fraction (vol%) of buriti fabric in epoxy composites as the MAS second layer value of plain epoxy (0 vol%) previously reported [59,63].

Together with the BFS vs. vol% graph in Figure 6, a bar corresponding to the value of Kevlar (22.7 ± 2.8 mm) as the MAS second layer with the same 10 mm thickness is shown for comparison from results reported elsewhere [63].

A slight tendency of increasing the BFS with the volume fraction of buriti fabric can be noticed in Figure 6. However, the standard deviations, shown as error interval for each average point, cast doubt on the possible differences between composites. The ANOVA in Table 3 was performed to elucidate this doubt. In this table, the degree of freedom (DF) corresponds to the minimum number of independent parameters. The total DF is $n \times k - 1$, where n is the number if treatments and k the number of samples. The residual DF is the difference between the total and treatment DF values.

Table 3. Analysis of variance (ANOVA) and Tukey test applied to ballistic BFS results with 7.62 mm ammunition of epoxy composites reinforced with buriti fabric in Figure 6.

	Variation Causes	Sum of Squares	DF	Mean of Squares	F_{calc}	F_{crit}	*p*-Value
ANOVA	Treatment	210.88	3	70.29	11.82	2.90	2.26×10^{-5}
	Residual	190.37	32	5.95			
	Total	401.24	35				
Tukey Test	**DF (Residual)**		**q (Tabled)**		***MSR***		***HSD***
	32		3.84		5.95		2.96

As presented in Table 3, a significant difference in the average values of BFS is confirmed through ANOVA and Tukey statistical analyses. According to this table, the $F_{cal} > F_{crit}$, which indicates with 95% level of confidence that the EC10BF composite exhibited the lowest BFS. On the other hand, the 20 and 30 vol% buriti fabric reinforced epoxy composites, as well as the previously found plain epoxy, are equal, since the obtained *HSD* was 2.96 mm (Table 3), and all the pair comparisons above this value are considered statistically different. Therefore, in principle, both EC20BF and EC30BF composites, and the plain epoxy, are as equally effective as the MAS second layer against the threat of a high velocity 7.62 mm projectile. It is worth mentioning, however, that only the composite reinforced with 30 vol% buriti fabric keeps complete integrity, Figure 5d, which guarantees protection against further shooting, as required by the NIJ standard 010106 [55]. On the contrary, plain epoxy and composites reinforced with 10 and 20 vol% of buriti fabric are extensively ruptured [54,63] and cannot be considered as the MAS second layer against a similar threat.

3.2. Stand-Alone Ballistic Tests

Table 4 presents the results of impact (v_i) and residual (v_r) velocities, as well as absorbed ballistic impact energy (E_{abs}) and limit velocity (V_L), for a stand-alone ballistic test against 7.62 mm ammunition. In addition, previous results of the same thickness (10 mm) plain epoxy and Kevlar plates [59,63] are also disclosed in Table 4.

Table 4. Results and parameter from 7.62 mm ballistic stand-alone tests for buriti fabric reinforced epoxy composites compared with reported results for plain epoxy and Kevlar.

Stand-Alone 10 mm Thick Plate Target	v_i **(m/s)**	v_r **(m/s)**	E_{abs} **(J)**	V_L **(m/s)**	**Ref.**
EC10BF	844 ± 6	824 ± 9	163 ± 46	182 ± 24	PW
EC20BF	840 ± 7	818 ± 6	178 ± 54	190 ± 30	PW
EC30BF	845 ± 9	823 ± 10	189 ± 50	194 ± 97	PW
DGEBA/TETA epoxy	850 ± 2	827 ± 6	190 ± 61	196 ± 32	[50]
Kevlar (ply of aramid fabric)	848 ± 6	841 ± 7	58 ± 29	109 ± 7	[49]

The variation in E_{abs} vs. volume fraction of buriti fabric in the epoxy composites is shown in Figure 7. In this figure, the value reported for the plain epoxy target is also exhibited [63] and the value of Kevlar (58 ± 29 J) with the same 10 mm thickness is also disclosed for comparison [59].

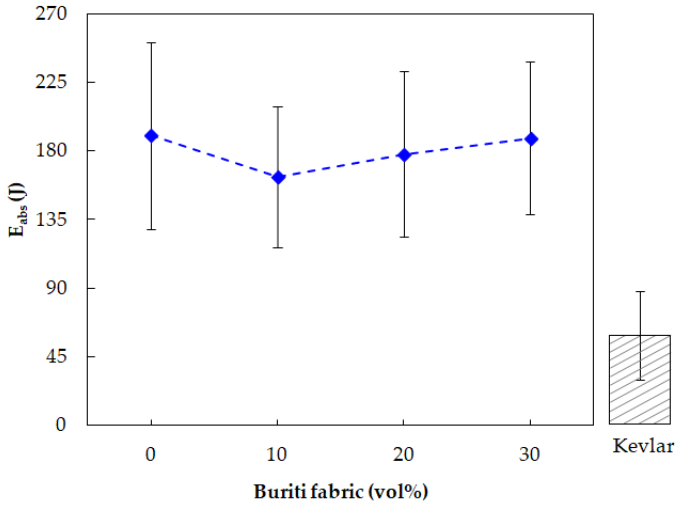

Figure 7. Variation of E_{abs} with the volume fraction (vol%) of buriti fabric in epoxy composites in stand-alone tests.

According to ANOVA in Table 5, it can be stated, with a 95% level of confidence, that the results of absorbed energy (E_{abs}) in stand-alone ballistic tests of buriti fabric reinforced composites as well as previously reported E_{abs} of plain epoxy [63] are statistically similar, since $F_{cal} < F_{crit}$. On the other hand, the E_{abs} value of 58 J for Kevlar, shown in the separated bar in Figure 7, is significantly lower than those exhibited for buriti/epoxy composites and plain epoxy (163 up to 190 J). Therefore, this may indicate that both epoxy and its buriti fabric composites as the second MAS layer dissipate ballistic impact energy more efficiently than Kevlar of the same thickness, which is further discussed in association with SEM failure analysis.

Table 5. Analysis of variance (ANOVA) of E_{abs} in a stand-alone ballistic test of buriti fabric composites and plain epoxy.

Variation Causes	Sum of Squares	DF	Mean of Squares	F_{calc}	F_{crit}	*p*-Value
Treatment	4275.82	3	1425.27	0.29	3.01	0.83
Residual	116,822.50	24	4867.60			
Total	121,098.32	27				

3.3. Scanning Electron Microscopy (SEM) Failure Analyses

As shown in Figure 5, both 10 and 20 vol% buriti fabric epoxy composites as the MAS second layer display a piercing failure. The observation of this failure in the 10 vol% buriti fabric composites by SEM is presented in Figure 8. Clear evidence of delamination between the buriti fiber (from the fabric) and the epoxy matrix is depicted in Figure 8a. The final undesirable effect of this delamination and some broken fibers at the perforated regions, pointed by red arrows in Figure 5b, are revealed in Figure 8b. Similar pictures were also obtained for the piercing cracks, pointed by yellow arrows in Figure 5c, for the 20 vol% buriti fabric composites.

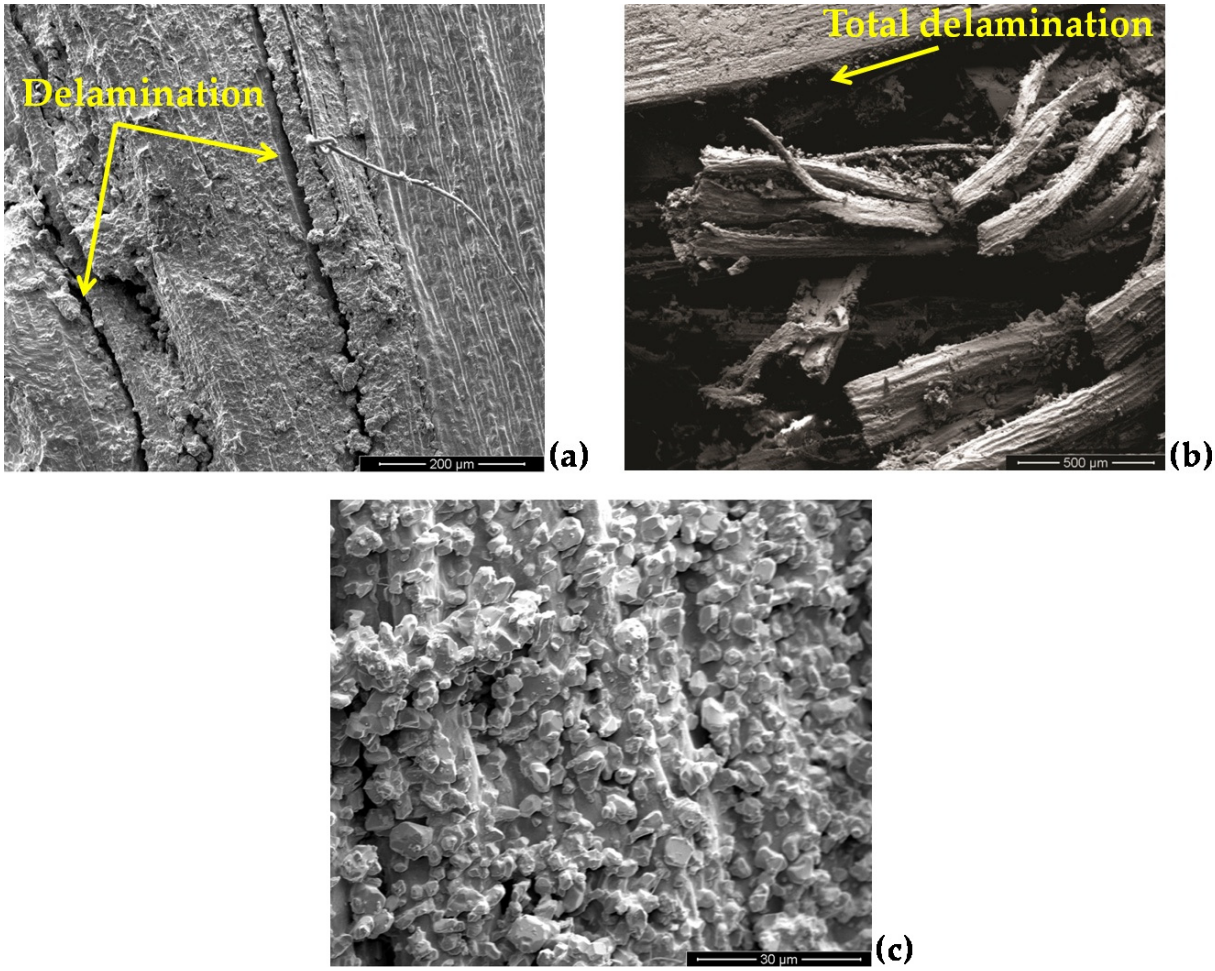

Figure 8. SEM images of the failure in a 10 vol% buriti fabric composite: (**a**) delamination; (**b**) total delamination and broken fibers; and (**c**) capture of ceramic fragments.

However, no apparent failure of any kind occurred for the 30 vol% buriti fabric composites illustrated in Figure 5d. One might then infer that this volume fraction of buriti fabric might be considered a lower limit to prevent large scale separation to occur between the fabric and the epoxy matrix. Indeed, as shown in Table 4 and Figure 7, despite the same absorbed ballistic energy, the epoxy composite with 30 vol% buriti fabric (EC30BF) is the only one that kept complete integrity without cracks or extensive open rupture, as revealed in Figure 5. Consequently, among the investigated composites, only EC30BF was not destroyed after the first 7.62 mm projectile impact and may stand integer in subsequent impacts as required by the NIJ standard [55]. Assuming that this behavior is a consequence of buriti fabric preventing the large-scale propagation of cracks or extensive rupture, it is then proposed that 30 vol% buriti be a lower limit for epoxy composites as the MAS second layer.

The favorable BFS of all buriti fabric composites, which are comparable to that of Kevlar [56] and much better than Dyneema [57] in Figure 6, can be attributed to the capacity of natural [63] and synthetic [13] fibers to capture fragments in the cloud resulting from a 7.62 mm projectile impact against the ceramic front layer.

To illustrate the magnitude of this cloud of ceramic fragments captured by the buriti fabric, Figure 8c shows the huge number of ceramic particles adhered to the surface of a buriti fiber. The presence of these ceramic fragments in the composite surface is attributed to van der Waals force and electrostatic attraction [28]. This mechanism not only contributes to the relatively low BFS in Figure 6 but also to the higher absorbed energy by the composites as compared to Kevlar in Figure 7.

It is worth mentioning another relevant point toward the application of NLFs composites as a MAS second layer in ballistic tests. The relatively lower density of these composites, compared to the ceramic front layer, results in lower shock-wave impedance since this is directly proportional to the density of the material. Then, when the compressive shock wave of the projectile impact at the interface of the ceramic/composite, a tensile wave is reflected, causing frontal ceramic shattering by dynamic fracture. Therefore, in general, a lower density material as a second layer MAS promotes a higher amplitude tensile wave, resulting in more energy dissipation [28].

4. Summary and Conclusions

Based on a previous study on the ballistic performance of a 10 vol% buriti (*Mauritia flexuosa*) natural fabric reinforced epoxy composite as a component of a multilayered armor system (MAS), which displayed satisfactory backface signature (BFS) but did not keep the required integrity, this work successfully increased the amount of buriti fabric to 30 vol%.

Against the threat of NIJ standard level III 7.62 mm rifle ammunition, the BFS of MAS with 10 mm thick both front ceramic and 30 vol% buriti fabric composites as the second layer was 25.0 mm, well below the lethal value of 44 mm specified by the standard.

Different than 10 and 20 vol% buriti fabric epoxy components, the 30 vol% buriti fabric composites kept their integrity, as required by the standard in multi-hit ballistic tests for personal protection.

In ballistic stand-alone tests, the 30 vol% buriti fabric composite disclosed values of absorbed energy, 189 J, and limit velocity for perforation, 194 m/s, superior to any other buriti fabric composite and Kevlar with the same thickness.

Delamination between buriti fabric and the epoxy matrix, which was the main mechanism of failure in 10 and 20 vol% buriti fabric composites, as found by SEM, was not observed in the 30 vol% buriti fabric composites. Herein, it is proposed that 30 vol% is the minimum amount that still guarantees the application of buriti fabric epoxy composites as the MAS second layer against the threat of a 7.62 mm projectile, assuring its integrity with a ballistic performance superior to both Kevlar and Dyneema.

Author Contributions: Conceptualization, data curation, investigation, methodology, L.C.d.C.D.; formal analysis, validation, writing—original draft, and writing—review and editing, F.S.d.L.; conceptualization, data curation, and visualization, L.F.C.N.; funding acquisition, project administration, and writing—review and editing, S.N.M. All authors have read and agreed to the published version of the manuscript.

Funding: This research was partially financed by the Coordination for the Improvement of Higher Education Personnel (CAPES), Brazil—Finance Code 001, Carlos Chagas Filho Foundation for Research Support of the State of Rio de Janeiro (FAPERJ) process E-26/202.286/2018, and the Brazilian National Council of Scientific Technological and Innovation Development (CNPq) grant number 423462/2018-0.

Institutional Review Board Statement: Not applicable.

Informed Consent Statement: Not applicable.

Data Availability Statement: Not applicable.

Acknowledgments: The authors would like to thank the Brazilian agencies CNPq, CAPES and FAPERJ (process E-26/202.286/2018) for their support.

Conflicts of Interest: The authors declare no conflict of interest.

References

1. Zhao, Z.; Liu, W.; Jiang, Y.; Wan, Y.; Du, R.; Li, H. Solidification of heavy metals in lead smelting slag and development of cementitious materials. *J. Clean. Prod.* **2022**, *359*, 132134. [CrossRef]
2. Ramos, F.J.H.T.V.; Marques, M.D.F.V.; Rodrigues, J.G.P.; de Oliveira Aguiar, V.; da Luz, F.S.; de Azevedo, A.R.G.; Monteiro, S.N. Development of novel geopolymeric foam composites coated with polylactic acid to remove heavy metals from contaminated water. *Case Stud. Constr. Mater.* **2022**, *16*, e00795. [CrossRef]

3. Zhang, S.; Jia, Z.; Cheng, B.; Zhao, Z.; Lu, F.; Wu, G. Recent progress of perovskite oxides and their hybrids for electromagnetic wave absorption: A mini-review. *Adv. Compos. Mater.* **2022**, 1–21. [CrossRef]
4. Song, Y.; Liu, X.; Gao, Z.; Wang, Z.; Hu, Y.; Yang, K.; Wu, G. Core-shell Ag@ C spheres derived from Ag-MOFs with tunable ligand exchanging phase inversion for electromagnetic wave absorption. *J. Colloid Interface Sci. Commun.* **2022**, *620*, 263–272. [CrossRef]
5. Liu, Y.; Jia, Z.; Zhan, Q.; Dong, Y.; Xu, Q.; Wu, G. Magnetic manganese-based composites with multiple loss mechanisms towards broadband absorption. *Nano Res.* **2022**, *15*, 5590–5600. [CrossRef]
6. Liu, Y.; Zhou, X.; Jia, Z.; Wu, H.; Wu, G. Oxygen Vacancy-Induced Dielectric Polarization Prevails in the Electromagnetic Wave-Absorbing Mechanism for Mn-Based MOFs-Derived Composites. *Adv. Funct. Mater.* **2022**, 2204499. [CrossRef]
7. Jia, Z.; Kong, M.; Yu, B.; Ma, Y.; Pan, J.; Wu, G. Tunable Co/ZnO/C@ MWCNTs based on carbon nanotube-coated MOF with excellent microwave absorption properties. *J. Mater. Sci. Technol.* **2022**, *127*, 153–163. [CrossRef]
8. Silva Chagas, N.P.; Aguiar, V.O.; Garcia Filho, F.C.; Figueiredo, A.B.H.S.; Monteiro, S.N.; Huaman, N.R.C.; Marques, M.D.F.V. Ballistic performance of boron carbide nanoparticles reinforced ultra-high molecular weight polyethylene (UHMWPE). *J. Mater. Res. Technol.* **2022**, *17*, 1799–1811. [CrossRef]
9. Meliande, N.M.; Silveira, P.H.P.M.D.; Monteiro, S.N.; Nascimento, L.F.C. Tensile Properties of Curaua—Aramid Hybrid Laminated Composites for Ballistic Helmet. *Polymers* **2022**, *14*, 2588. [CrossRef]
10. Costa, U.O.; Nascimento, L.F.C.; Bezerra, W.B.A.; Neves, P.P.; Huaman, N.R.C.; Monteiro, S.N.; Pinheiro, W.A. Dynamic and Ballistic Performance of Graphene Oxide Functionalized Curaua Fiber-Reinforced Epoxy Nanocomposites. *Polymers* **2022**, *14*, 1859. [CrossRef]
11. Medvedovski, E. Ballistic performance of armour ceramics: Influence of design and structure. Part 1. *Ceram. Int.* **2010**, *36*, 2103–2115. [CrossRef]
12. Medvedovski, E. Ballistic performance of armour ceramics: Influence of design and structure. Part 2. *Ceram. Int.* **2010**, *36*, 2117–2127. [CrossRef]
13. Tasdemirci, A.; Tunusoglu, G.; Güden, M. The effect of the interlayer on the ballistic performance of ceramic/composite armors: Experimental and numerical study. *Int. J. Impact Eng.* **2012**, *44*, 1–9. [CrossRef]
14. Lee, Y.S.; Wetzel, E.D.; Wagner, N.J. The Ballistic Impact Characteristic of kevlar woven fabrics impregnated with a colloidal shear thickening fluid. *J. Mater. Sci.* **2003**, *38*, 2825–2833. [CrossRef]
15. Odesanya, K.O.; Ahmad, R.; Jawaid, M.; Bingol, S.; Adebayo, G.O.; Wong, Y.H. Natural fibre-reinforced composite for ballistic applications: A review. *J. Polym. Environ.* **2021**, *29*, 3795–3812. [CrossRef]
16. Nurazzi, N.M.; Asyraf, M.R.M.; Khalina, A.; Abdullah, N.; Aisyah, H.A.; Rafiqah, S.; Sabaruddin, F.A.; Kamarudin, S.H.; Norrrahim, M.N.F.; Ilyas, A.; et al. A review on natural fiber reinforced polymer composite for bullet proof and ballistic applications. *Polymers* **2021**, *13*, 646. [CrossRef]
17. Nayak, S.Y.; Sultan, M.T.H.; Shenoy, S.B.; Kini, C.R.; Samant, R.; Shah, A.U.M.; Amuthakkannan, P. Potential of natural fibers in composites for ballistic applications—A review. *J. Nat. Fibers* **2021**, *19*, 1–11. [CrossRef]
18. Gholampour, A.; Ozbakkaloglu, T. A review of natural fiber composites: Properties, modification and processing techniques, characterization, applications. *J. Mater. Sci.* **2020**, *55*, 829–892. [CrossRef]
19. Araújo, E.M.; Araújo, K.D.; Pereira, O.D.; Ribeiro, P.C.; Melo, T.J. Fiberglass wastes/polyester resin composites: Mechanical properties and water sorption. *Polímeros* **2006**, *16*, 332–335. [CrossRef]
20. Bindal, A.; Singh, S.; Batra, N.K.; Khanna, R. Development of glass/jute fibers reinforced polyester composite. *Indian J. Mater. Sci.* **2013**, *2013*, 675264. [CrossRef]
21. Aisyah, H.A.; Paridah, M.T.; Sapuan, S.M.; Ilyas, R.A.; Khalina, A.; Nurazzi, N.M.; Lee, S.H.; Lee, C.H. A comprehensive review on advanced sustainable woven natural fibre polymer composites. *Polymers* **2021**, *13*, 471. [CrossRef] [PubMed]
22. Zhang, Z.; Cai, S.; Li, Y.; Wang, Z.; Long, Y.; Yu, T.; Shen, Y. High performances of plant fiber reinforced composites—A new insight from hierarchical microstructures. *Compos. Sci. Technol.* **2020**, *194*, 108151. [CrossRef]
23. Güven, O.; Monteiro, S.N.; Moura, E.A.B.; Drelich, J.W. Re-emerging field of lignocellulosic fiber-polymer composites and ionizing radiation technology in their formulation. *Polym. Rev.* **2016**, *56*, 706–736. [CrossRef]
24. Monteiro, S.N.; Lopes, F.P.D.; Ferreira, A.S.; Nascimento, D.C.O. Natural-fiber polymer-matrix composites: Cheaper, tougher, and environmentally friendly. *JOM* **2009**, *61*, 17–22. [CrossRef]
25. Dunne, R.; Desai, D.; Sadiku, R.; Jayaramudu, J. A review of natural fibres, their sustainability and automotive applications. *J. Reinf. Plast. Compos.* **2016**, *35*, 1041–1050. [CrossRef]
26. Kumar, R.; Ul-Haq, M.I.; Raina, A.; Anand, A. Industrial applications of natural fibre-reinforced polymer composites–challenges and opportunities. *Int. J. Sustain. Eng.* **2019**, *12*, 212–220. [CrossRef]
27. Islam, M.S.; Ahmed, S.J. Influence of jute fiber on concrete properties. *Constr. Build. Mater.* **2018**, *189*, 768–776. [CrossRef]
28. Monteiro, S.N.; Lopes, F.P.D.; Costa, L.L.; Motta, L.C.; Santos, L.F.L., Jr. Study of the buriti waste fiber as a possible reinforcement of polyester composites. In Proceedings of the REWAS 2008: Global Symposium on Recycling, Waste Treatment and Clean Technology, Cancun, Mexico, 12–15 October 2008; pp. 517–522.
29. Portela, T.G.R.; da Costa, L.L.; Santos, N.S.S.; Lopes, F.P.D.; Monteiro, S.N. Tensile behavior of lignocellulosic fiber reinforced polymer composites: Part II buriti petiole/polyester. *Matéria* **2010**, *15*, 195–201. [CrossRef]
30. Santos, R.S.; de Souza, A.A.; De Paoli, M.A.; de Souza, C.M.L. Cardanol—Formaldehyde thermoset composites reinforced with buriti fibers: Preparation and characterization. *Compos. Part A Appl. Sci. Manuf.* **2010**, *41*, 1123–1129. [CrossRef]

31. Demosthenes, L.C.C.; Nascimento, L.F.C.; Monteiro, S.N.; Costa, U.O.; Garcia Filho, F.C.; Luz, F.S.; Oliveira, M.S.; Ramos, F.J.H.T.V.; Pereira, A.C.; Braga, F.O. Thermal and structural characterization of buriti fibers and their relevance in fabric reinforced composites. *J. Mater. Res. Technol.* **2020**, *9*, 115–123. [CrossRef]
32. Portela, T.G.R.; da Costa, L.L.; Santos, N.S.S.; Lopes, F.P.D.; Monteiro, S.N. Tensile strength of polymeric composites reinforced with aligned buriti fibers. In Proceedings of the 1st TMS/ABM International Materials Congress, Rio de Janeiro, Brazil, 26–30 July 2010; Volume 3, pp. 2439–2446, ISBN 978-1-61782-016-8.
33. Portela, T.G.R.; Costa, L.L.; Loiola, R.L.; Monteiro, S.N. Flexural mechanical characterization of polyester composites reinforced with continuous buriti petiole fibers. In *EPD Congress 2011*; John Wiley & Sons, Inc.: Hoboken, NJ, USA, 2011; Volume 1, pp. 311–318. ISBN 978-1-11803-652-5. [CrossRef]
34. Altoé, G.R.; Loiola, R.L.; Margem, F.M.; Simonassi, N.T.; Monteiro, S.N. Tensile behavior of epoxy composites reinforced with continuous and thinner buriti fibers. *Charact. Miner. Met. Mater.* **2013**, *15*, 159–165. [CrossRef]
35. Monteiro, S.N.; Muylaert Margem, F.; Oliveira, M.P.; Altoé, G.R. Izod impact tests with polyester matrix reinforced with buriti fibers. *Mater. Sci. Forum* **2014**, *775–776*, 330–335. [CrossRef]
36. Altoé, G.R.; Margem, F.M.; Monteiro, S.N.; Faria, R.T., Jr.; Cordeiro, T.C. Thermal characterization of epoxy matrix reinforced with buriti fibers by the photoacoustic technique. In *TMS 2014 143rd Annual Meeting & Exhibition, Annual Meeting Supplemental Proceedings*; Wiley: Hoboken, NJ, USA, 2014; Volume 441–448, ISBN 978-1-118-88786-8.
37. Monteiro, S.N.; Margem, F.M.; Altoé, G.R.; Loiola, R.L.; Oliveira, M.P. Tensile strength of polyester composites reinforced with thinner buriti fibers. *Mater. Sci. Forum* **2014**, *775–776*, 183–188. [CrossRef]
38. Barbosa, A.D.; Oliveira, M.P.; Altoé, G.R.; Margem, F.M.; Monteiro, S.N. Charpy impact test of epoxy matrix composites reinforced with buriti fibers. *Mater. Sci. Forum* **2014**, *775–776*, 296–301. [CrossRef]
39. Barbosa, A.D.; Oliveira, M.P.; Altoé, G.R.; Margem, F.M.; Monteiro, S.N. Manufacturing of epoxy composites incorporated with buriti fibers and evaluation of thermogravimetric behavior. *Mater. Sci. Forum* **2015**, *805*, 460–465. [CrossRef]
40. Barbosa, A.D.P.; Altoé, G.R.; Loiola, R.L.; Margem, F.M.; Braga, F.O.; Monteiro, S.N. Bending mechanical behavior of epoxy matrix reinforced with buriti fiber. *Mater. Sci. Forum* **2016**, *869*, 243–248. [CrossRef]
41. Pelegrini, K.; Donazzolo, I.; Brambilla, V.; Coulon Grisa, A.M.; Piazza, D.; Zattera, A.J.; Brandalise, R.N. Degradation of PLA and PLA in composites with triacetin and buriti fiber after 600 days in a simulated marine environment. *J. Appl. Polym. Sci.* **2016**, *133*, 43290. [CrossRef]
42. Brambilla, V.C.; Beltrami, L.V.; Pelegrini, K.; Zimmermann, M.V.; Brandalise, R.N.; Zattera, A.J. Development and characterization of PLA/buriti fibre composites–influence of fibre and coupling agent contents. *Polym. Polym. Compos.* **2017**, *25*, 143–152. [CrossRef]
43. Lavoratti, A.; Romanzini, D.; Amico, S.C.; Zattera, A.J. Influence of fibre treatment on the characteristics of buriti and ramie polyester composites. *Polym. Polym. Compos.* **2017**, *25*, 247–256. [CrossRef]
44. Satyanarayana, K.G.; Guimarães, J.L.; Wypych, F. Studies on lignocellulosic fibers of Brazil. Part I: Source, production, morphology, properties and applications. *Compos. Part A* **2007**, *38*, 1694–1709. [CrossRef]
45. Vieira, D.A.; Facó, L.R.; Cecy, A. Buriti: A savanna like vegetation fruit considered a multiple usage plant. *Cenarium Pharmacêutico* **2011**, *4*, 11–22. (In Portuguese)
46. Monteiro, S.N.; Lopes, F.P.D.; Barbosa, A.P.; Bevitori, A.B.; Silva, I.L.A.; Costa, L.L. Natural lignocellulosic fibers as engineering materials—An overview. *Metall. Mater. Trans. A* **2011**, *42*, 2963–2974. [CrossRef]
47. Monteiro, S.N.; Braga, F.O.; Lima, E.P., Jr.; Louro, L.H.L.; Drelich, J.W. Promising curaua fiber-reinforced polyester composite for high-impact ballistic multilayered armor. *Polym. Eng. Sci.* **2017**, *57*, 947–954. [CrossRef]
48. Braga, F.O.; Bolzan, L.T.; Lima, É.P., Jr.; Monteiro, S.N. Performance of natural curaua fiber-reinforced polyester composites under 7.62 mm bullet impact as a stand-alone ballistic armor. *J. Mater. Res. Technol.* **2017**, *6*, 323–328. [CrossRef]
49. Silva, A.O.; Monsores, K.G.C.; Oliveira, S.D.S.A.; Weber, R.P.; Monteiro, S.N. Ballistic behavior of a hybrid composite reinforced with curaua and aramid fabric subjected to ultraviolet radiation. *J. Mater. Res. Technol.* **2018**, *7*, 584–591. [CrossRef]
50. Costa, U.O.; Nascimento, L.F.C.; Garcia, J.M.; Monteiro, S.N.; Luz, F.S.; Pinheiro, W.A.; Garcia Filho, F.C. Effect of graphene oxide coating on natural fiber composite for multilayered ballistic armor. *Polymers* **2019**, *11*, 1356. [CrossRef]
51. Reis, R.H.M.; Nunes, L.F.; Luz, F.S.; Candido, V.S.; Silva, A.C.R.; Monteiro, S.N. Ballistic performance of guaruman fiber composites in multilayered armor system and as single target. *Polymers* **2021**, *13*, 1203. [CrossRef]
52. Oliveira, M.S.; Luz, F.S.; Souza, A.T.; Demosthenes, L.C.C.; Pereira, A.C.; Braga, F.O.; Figueiredo, A.B.H.S.; Monteiro, S.N. Tucum fiber from Amazon *Astrocaryum vulgare* palm tree: Novel reinforcement for polymer composites. *Polymers* **2020**, *12*, 2259. [CrossRef]
53. Demosthenes, L.C.C.; Nascimento, L.F.C.; Oliveira, M.S.; Garcia Filho, F.C.; Pereira, A.C.; da Luz, F.S.; Lima, É.P.; Demosthenes, L.A.C.; Monteiro, S.N. Evaluation of buriti fabric as reinforcement of polymeric matrix composite for ballistic application as multilayered armor system. In *Green Materials Engineering*; Ikhmayies, S., Li, J., Vieira, C., Margem, J.I., Braga, F.O., Eds.; Springer—TMS: Cham, Switzerland, 2019; pp. 177–183. [CrossRef]
54. Monteiro, S.N.; Lima, E.P., Jr.; Louro, L.H.L.; Silva, L.C.; Drelich, J.W. Unlocking function of aramid fibers in multilayered ballistic armor. *Metall. Mater. Trans. A* **2014**, *46*, 37–40. [CrossRef]

55. National Criminal Justice Reference Service. US Department of Justice, & National Institute of Justice. NIJ 0101.06. Ballistic Resistance of Body Armor. 2008. Available online: https://nij.ojp.gov/library/publications/ballistic-resistance-body-armor-nij-standard-010106 (accessed on 15 May 2021).
56. Monteiro, S.N.; Milanezi, T.L.; Louro, L.H.L.; Lima, E.P.; Braga, F.O.; Gomes, A.V.; Drelich, J.W. Novel ballistic ramie fabric composite competing with kevlarTM fabric in multilayered armor. *Mater. Des.* **2016**, *96*, 263–269. [CrossRef]
57. Luz, F.S.; Garcia Filho, F.C.; Oliveira, M.S.; Nascimento, L.F.C.; Monteir, S.N. Composites with natural fibers and conventional materials applied in a hard armor: A comparison. *Polymers* **2020**, *12*, 1920. [CrossRef] [PubMed]
58. Braga, F.O.; Bolzan, L.T.; Luz, F.S.; Lopes, P.H.L.M.; Lima, E.P., Jr.; Monteiro, S.N. High energy ballistic and fracture comparison between multilayered armor systems using non-woven curaua fabric composites and aramid laminates. *J. Mater. Res. Technol.* **2017**, *6*, 417–422. [CrossRef]
59. Luz, F.S.; Lima Junior, E.P.; Louro, L.H.L.; Monteiro, S.N. Ballistic test of multilayered armor with intermediate epoxy composite reinforced with jute fabric. *Mater. Res.* **2015**, *18*, 170–177. [CrossRef]
60. Ribeiro, M.P.; Neuba, L.M.; da Silveira, P.H.P.M.; da Luz, F.S.; da Silva Figueiredo, A.B.H.; Monteiro, S.N.; Moreira, M.O. Mechanical, thermal and ballistic performance of epoxy composites reinforced with *Cannabis sativa* hemp fabric. *J. Mater. Res. Technol.* **2021**, *12*, 221–233. [CrossRef]
61. Santos, J.L.; Marçal, R.L.S.B.; Jesus, P.R.R.; Gomes, A.V.; Lima, E.P.; Monteiro, S.N.; Capos, J.B.; Louro, L.H.L. Effect of LiF as sintering agent on the densification and phase formation in Al_2O_3-4wt % Nb_2O_5 ceramic compound. *Metall. Mater. Trans. A* **2017**, *48*, 4432–4440. [CrossRef]
62. Morye, S.S.; Hine, P.J.; Duckett, R.A.; Carr, D.J.; Ward, I.M. Modelling of the energy absorption by polymer composites upon ballistic impact. *Compos. Sci. Technol.* **2000**, *60*, 2631–2642. [CrossRef]
63. Monteiro, S.N.; Louro, L.H.L.; Trindade, W.; Elias, C.N.; Ferreira, C.L.; de Sousa Lima, E.; Weber, R.P.; Suarez, J.C.; Figueiredo, A.B.H.S.; Pinheiro, W.A.; et al. Natural curaua fiber-reinforced composites in multilayered ballistic armor. *Metall. Mater. Trans. A* **2015**, *46*, 4567–4577. [CrossRef]